Synthesis and Structures of Mesitylgallylene-Bridged Diiron Complexes $[Cp'Fe(CO)]_2(\mu\text{-CO})(\mu\text{-GaMes})$ ($Cp' = \eta\text{-}C_5Me_5$, $\eta\text{-}C_5H_5$; Mes = 2,4,6-Trimethylphenyl) and Kinetic Study of the Cis−Trans Isomerization of $[(\eta\text{-}C_5H_5)Fe(CO)]_2(\mu\text{-CO})(\mu\text{-GaMes})$

Takeshi Yamaguchi, Keiji Ueno,* and Hiroshi Ogino*

Department of Chemistry, Graduate School of Science, Tohoku University, Sendai 980-8578, Japan

Received August 7, 2000

Gallylene-bridged diiron complexes $[Cp'Fe(CO)_2]_2(\mu\text{-GaMes})$ ($Cp' = \eta\text{-}C_5Me_5$ (**1a**), $\eta\text{-}C_5H_5$ (**1b**); Mes = 2,4,6-trimethylphenyl) were synthesized by the reactions of $M[Cp'Fe(CO)_2]$ (M = K, Na) with $MesGaCl_2$ in THF. Photolysis of a toluene solution of complex **1a** resulted in the formation of the trans isomer of the gallylene- and carbonyl-bridged diiron complex $[Cp^*Fe(CO)]_2(\mu\text{-CO})(\mu\text{-GaMes})$ (**2a**: $Cp^* = \eta\text{-}C_5Me_5$), in which the two Cp* rings are located on the opposite side with respect to the $GaFe_2C$ four-membered ring. In contrast to **1a**, photolysis of a toluene solution of **1b** afforded a mixture of the cis and trans isomers of $[CpFe(CO)]_2(\mu\text{-CO})(\mu\text{-GaMes})$ (**2b**: $Cp = \eta\text{-}C_5H_5$). Recrystallization of **2b** from a toluene/hexane solution afforded pure *trans*-**2b**. Crystal structure analyses of **1a**, **2a**, and *trans*-**2b** revealed that the Fe−Ga distances of **2a** (2.3147(9) Å) and *trans*-**2b** (2.3438(5) Å) are much shorter than those of **1a** (2.4315(15) Å). A kinetic investigation of the isomerization between *cis*-**2b** and *trans*-**2b** afforded the activation parameters (trans → cis: $\Delta H^{\ddagger} = 102(1)$ kJ mol^{-1}, $\Delta S^{\ddagger} = 36(4)$ J K^{-1} mol^{-1}, $\Delta G^{\ddagger}_{298} = 91(2)$ kJ mol^{-1}; cis → trans: $\Delta H^{\ddagger} = 105(2)$ kJ mol^{-1}, $\Delta S^{\ddagger} = 52(5)$ J K^{-1} mol^{-1}, $\Delta G^{\ddagger}_{298} = 90(3)$ kJ mol^{-1}). A possible mechanism is proposed for the isomerization which contains $[CpFe(CO)_2][CpFe(CO)](\mu\text{-GaMes})$ as a key intermediate.

Introduction

The monovalent organogallium species gallylene (GaR) is of inherent interest as a bridging ligand owing to the isolobal relationship to a cationic carbyne, a neutral carbene, and the heavier congeners such as cationic silylyne and neutral silylene. However, the chemistry of gallylene-bridged transition-metal complexes, especially those with a three-coordinate gallium center, is less developed compared to that of silylene- and germylene-bridged complexes.[1] Structural studies of three-coordinate gallylene-bridged complexes have been limited to the following seven complexes: $[CpFe(CO)_2]_2(\mu\text{-GaBu}^t)$ (**3**),[2] $(PPN)_2[\{Fe(CO)_4\}_2(\mu\text{-GaMe})]$ (**4**, PPN = bis(triphenylphosphoranylidene)ammonium),[3] $[Co(CO)_4]_2\{\mu\text{-Ga}(2,4,6\text{-Bu}^t{}_3C_6H_2)\}$ (**5**),[4] $[Fe(CO)_3]_2\{\mu\text{-GaSi}(SiMe_3)_3\}_3$ (**6**),[5] $[Fe(CO)_3]_2\{\mu\text{-GaSi}(SiMe_3)_3\}_2(\mu\text{-CO})$ (**7**),[5] $[Mn(CO)_4]_2\{\mu\text{-GaC}(SiMe_3)_3\}_2$ (**8**),[6] and $[Fe(CO)_3]_3(\mu\text{-CO})\{\mu\text{-GaC}(SiMe_3)_3\}_2$ (**9**).[6]

In this paper, we report the synthesis and crystal structures of gallylene- and carbonyl-bridged diiron complexes with an iron−iron bond, $[Cp'Fe(CO)]_2(\mu\text{-CO})(\mu\text{-GaMes})$ (**2**). Complex **2** was obtained by photolysis of $[Cp'Fe(CO)]_2(\mu\text{-GaMes})$ (**1**), which has no iron−iron bond.

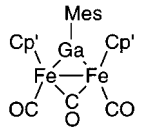

2

Results and Discussion

Synthesis of Gallylene- and Carbonyl-Bridged Diiron Complexes 2a and 2b. Gallylene is a highly electron deficient species. Thus a gallylene-bridged complex easily undergoes coordination by a two-electron donor to form a four-coordinate gallium species or decomposition via disproportionation unless the gallium center is stabilized sterically or electronically.[2,3] In this work, we used the bulky mesityl group to protect the gallylene-bridged diiron complexes. Complexes **1a** and **1b** were synthesized by the reaction of $M[Cp'Fe(CO)_2]$ (M = Na, K) with $MesGaCl_2$ in THF in 36 and 64% yield, respectively (eq 1).

(1) (a) Aylett, B. J. *Adv. Inorg. Chem. Radiochem.* **1982**, *25*, 1. (b) Tilley, T. D. In *The Chemistry of Organic Silicon Compounds*; Patai, S., Rappoport, Z., Eds.; John Wiley & Sons: New York, 1989; Chapter 24. (c) Ogino, H.; Tobita, H. *Adv. Organomet. Chem.* **1998**, *42*, 223.

(2) He, X.; Bartlett, R. A.; Power, P. P. *Organometallics* **1994**, *13*, 548.

(3) Fischer, R. A.; Schulte, M. M.; Herdtweck, E.; Mattner, M. R. *Inorg. Chem.* **1997**, *36*, 2010.

(4) Cowley, A. H.; Decken, A.; Olazábal, C. A.; Norman, N. *Inorg. Chem.* **1994**, *33*, 3435.

(5) Linti, G.; Køostler, W. *Chem. Eur. J.* **1998**, *4*, 942.

(6) Uhl, W.; Benter, M.; Prött, M. *J. Chem. Soc., Dalton Trans.* **2000**, 643.

10.1021/om000675a CCC: $20.00
Publication on Web 01/05/2001

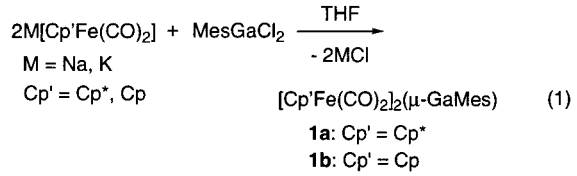

The solution IR spectrum of **1a** showed four ν_{CO} absorptions at 1973 (vs), 1942 (w), 1915 (vs), and 1900 (w) cm^{-1}, while that of **1b** showed three strong absorptions at 1996, 1967, and 1944 cm^{-1}. The observation of four ν_{CO} bands and their relative intensities for complex **1a** indicates that the molecule has C_2 symmetry,[7] which is consistent with the crystal structure (vide infra). Complex **1b**, in contrast to **1a**, has C_{2v} symmetry on the basis of the observation of three strong ν_{CO} absorptions.[7] The lower symmetry of **1a** is possibly caused by the large steric repulsion between the two Cp* ligands. The red shift of the ν_{CO} bands of **1a** compared to those of **1b** is attributable to the stronger electron-donating character of the Cp* ligand vs that of the Cp ligand, which causes stronger π-back-donation from the iron atom to the carbonyl ligands.[8]

Photolysis of a toluene solution of **1a** resulted in almost quantitative (by ^{1}H NMR) formation of a gallylene- and carbonyl-bridged diiron complex with an iron−iron bond, **2a** (eq 2), dark violet crystals in 40% yield. Its ^{1}H NMR spectrum showed singlets at 6.70,

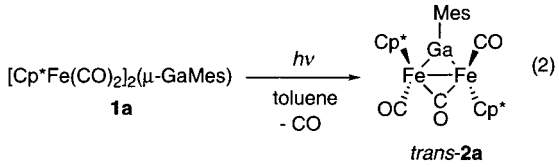

2.79, 2.23, and 1.71 ppm, which are assignable to the *m*-H, *o*-Me, and *p*-Me of the mesityl group and Cp*, respectively. For complex **2a**, cis and trans configurations are possible. However, the trans configuration is strongly suggested since the IR spectrum shows ν_{CO} bands at 1882 and 1734 cm^{-1}, which are assignable to the asymmetric stretching absorption of the terminal carbonyl ligands and the bridging carbonyl stretching absorption, respectively. No symmetric stretching vibration of the terminal carbonyl groups was observed. The trans configuration of **2a** was further confirmed by an X-ray crystal structure analysis (vide infra).

In contrast to **2a**, photolysis of a toluene solution of **1b** afforded a mixture of geometric isomers, *cis*-**2b** and *trans*-**2b** (eq 3). The IR spectrum of a THF solution of **2b** showed strong ν_{CO} bands at 1942, 1905, and 1751 cm^{-1}. The ν_{CO} absorption at 1942 cm^{-1} is assignable to the symmetric stretching vibration of the terminal carbonyl groups, which indicates the existence of the cis isomer. The ^{1}H NMR spectrum of complex **2b** showed two sets of signals in approximately 3:2 intensity ratio. The major isomer gave the Cp, *o*-Me, and *p*-Me signals

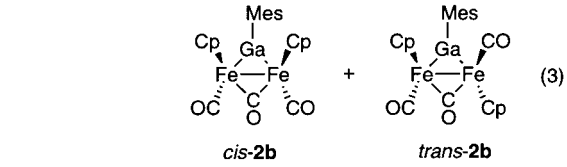

at 4.29, 2.58, and 2.21 ppm, respectively, whereas the minor one showed resonances at 4.14, 2.47, and 2.20 ppm. The major isomer was isolated as violet crystals upon crystallization from a toluene/hexane solution of the mixture of isomers and was confirmed to be *trans*-**2b** by X-ray crystal structure analysis (vide infra). In the *cis*-**2b**, the two *o*-Me groups as well as the two *m*-H atoms of the mesityl substituent could be inequivalent since the chemical environments are different between the Cp side and the terminal CO side of the Fe−Ga−Fe−C four-membered ring. However, only one ^{1}H NMR signal was observed for the *o*-Me groups and *m*-H atoms, respectively, even at low temperature (210 K). This suggests that the rotation of the mesityl group around the Ga−Mes bond occurs much faster than the NMR time scale and that the steric repulsion between the mesityl group and other part of the molecule is insignificant.

Kinetic Study of the Isomerization between *trans*-2b and *cis*-2b. Complex **2b** exists as an equilibrium mixture of two geometrical isomers, *trans*-**2b** and *cis*-**2b**, in solution (eq 4). When the crystals of *trans*-**2b**

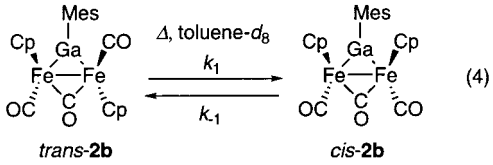

were dissolved in toluene-d_8, *trans*-**2b** isomerized gradually to *cis*-**2b** and an equilibrium was attained between *cis*-**2b** and *trans*-**2b** within several hours at room temperature. Figure 1 shows the ^{1}H NMR spectral change of a toluene-d_8 solution of *trans*-**2b** at 283 K. The signals assignable to the *trans*-**2b** decreased gradually with concomitant increase of those assignable to the *cis*-**2b**. The isomerization reaction was monitored by ^{1}H NMR spectroscopy at 273, 278, 283, 288, and 293 K. The equilibrium ratios and the equilibrium constants (K) between *cis*-**2b** and *trans*-**2b** and the rate constants (k_1 and k_{-1}) of cis−trans isomerization at various temperatures are summarized in Table 1 and activation parameters for the trans → cis and cis → trans isomerizations in Table 2. The $\Delta H^{\ddagger}$ values are comparable to the reported $\Delta H^{\ddagger}$ values for the isomerization of [CpFe(CO)]$_2$(μ-CO)(μ-E) (E = CR_2, SiR_2, GeR_2) (56−100 kJ mol^{-1}).[9,10] On the basis of the small $\Delta S^{\ddagger}$ values, a

(7) (a) Flitcroft, N.; Harbourne, D. A.; Paul, I.; Tucker, P. M.; Stone, F. G. A. *J. Chem. Soc. A* **1966**, 1130. (b) Hampden-Smith, M. J.; Lei, D.; Duesler, E. N. *J. Chem. Soc., Dalton Trans.* **1990**, 2953.

(8) (a) King, R. B.; Bisnette, M. B. *J. Organomet. Chem.* **1967**, *8*, 287. (b) Tobita, H.; Ueno, K.; Simoi, M.; Ogino, H. *J. Am. Chem. Soc.* **1990**, *112*, 3415. (c) Tellers, D. M.; Skoog, S. J.; Bergman, B. G.; Gunnoe, R. G.; Harman, W. D. *Organometallics* **2000**, *19*, 2428.

(9) (a) Altbach, M. I.; Muedas, C. A.; Korswagen, R. P. *J. Organomet. Chem.* **1986**, *306*, 375. (b) Kawano, Y.; Tobita, H.; Ogino, H. *Organometallics* **1992**, *11*, 499. (c) Ueno, K.; Hamashima, N.; Ogino, H. *Organometallics* **1992**, *11*, 1435. (d) El-Maradny, A.; Tobita, H.; Ogino, H. *Organometallics* **1996**, *15*, 4954. (e) Luh, L. S.; Wen, Y. S.; Tobita, H.; Ogino, H. *Bull. Chem. Soc. Jpn.* **1997**, *70*, 2193.

(10) (a) Adams, R. D.; Brice, M. D.; Cotton, F. A. *Inorg. Chem.* **1974**, *13*, 1080. (b) Casey, C. P.; Gable, K. P.; Roddick, D. M. *Organometallics* **1990**, *9*, 221.

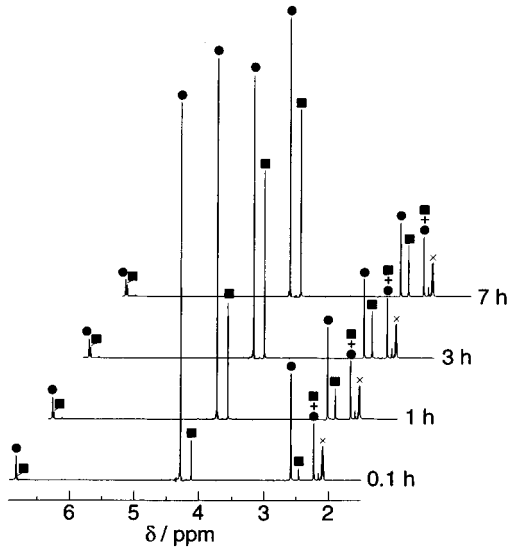

Figure 1. ^{1}H NMR spectral change of a toluene-d_8 solution of *trans*-**2b** at 283 K: (●) *trans*-**2b**; (■) *cis*-**2b**; (×) C_6D_5-CD_2H.

Table 1. Equilibrium Ratios, Equilibrium Constants, and Rate Constants for the Cis−Trans Isomerization of [CpFe(CO)]$_2$(*μ*-CO)(*μ*-GaMes) (2b)

T/K	[trans]/[cis]	*K*[a]	$k_1/10^{-5}$ s^{-1}	$k_{-1}/10^{-5}$ s^{-1}
273	60:40	0.66	1.6(1)	2.4(1)
278	61:39	0.65	3.7(1)	5.7(1)
283	61:39	0.64	7.8(1)	12(1)
288	62:38	0.62	18(1)	29(1)
293	63:37	0.60	37(1)	61(1)

[a] K = [cis]/[trans] = k_1/k_{-1}.

Table 2. Activation Parameters for the Isomerization between *trans*- and *cis*-[CpFe(CO)]$_2$(*μ*-CO)(*μ*-GaMes) (2b)

	trans → cis	cis → trans
$\Delta H^{\ddagger}$/kJ mol^{-1}	102(1)	105(2)
$\Delta S^{\ddagger}$/J K^{-1} mol^{-1}	36(4)	52(5)
$\Delta G^{\ddagger}_{298}$/kJ mol^{-1}	91(2)	90(3)

dissociative mechanism such as elimination of CO to form an intermediate, [CpFe(CO)][CpFe](*μ*-CO)(*μ*-GaMes), can be ruled out for the isomerization. This is also supported by the fact that complex **2b** did not react with PMe_3 in C_6D_6 at all, even upon heating the reaction mixture at 60 °C for 2 days.

Scheme 1 shows possible mechanisms for the isomerization. In path A, an Fe−(*μ*-CO) bond and an Fe−Fe bond of the trans isomer are cleaved to form the intermediate **A**, which retains the Fe−Ga−Fe framework.[11] Subsequent rotation of the CpFe(CO) fragment and cyclization produces the cis isomer. Another possible mechanism, path B, can be categorized as an Adams−Cotton mechanism, which was originally proposed for the cis−trans isomerization of [CpFe(CO)]$_2$(*μ*-CO)$_2$.[12] In this mechanism, the intermediate **B**, with a terminal gallylene ligand, was formed by moving the bridging gallylene and carbonyl ligands to the terminal positions.

(11) The 16-electron iron center in the CpFe(CO) fragment would be weakly coordinated by a solvent molecule, as proposed for the intermediate of the cis−trans isomerization of silylene-, germylene-, and carbene-bridged diiron complexes.[9]

(12) (a) Bullitt, J. G.; Cotton, F. A.; Marks, T. J. *J. Am. Chem. Soc.* **1970**, *92*, 2155. (b) Adams, R. D.; Cotton, F. A. *J. Am. Chem. Soc.* **1973**, *95*, 6589.

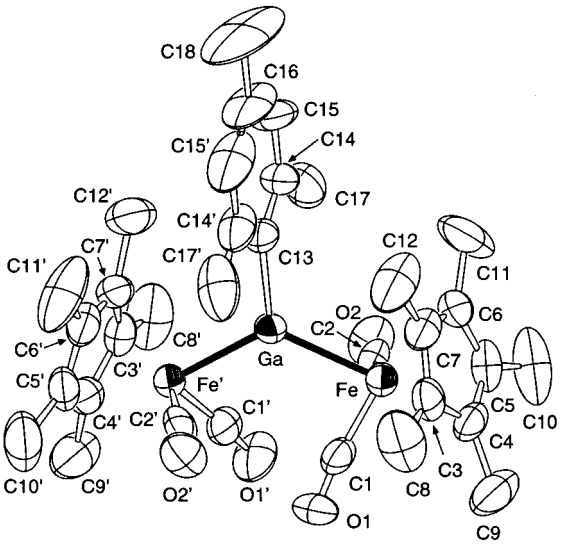

Figure 2. ORTEP drawing (50% probability level) of [Cp*Fe(CO)$_2$]$_2$(*μ*-GaMes) (**1a**).

Scheme 1

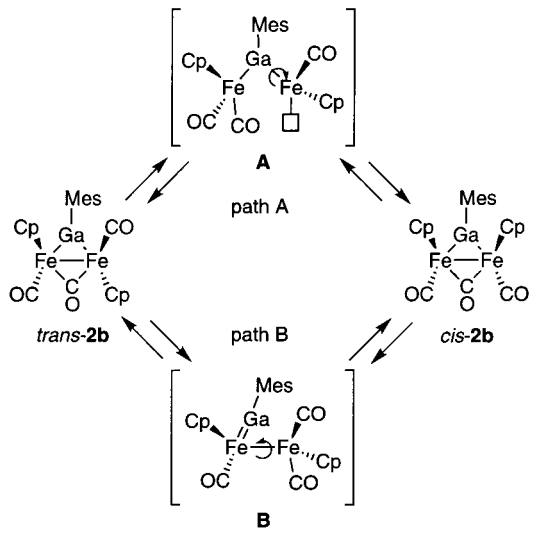

Rotation around the Fe−Fe bond followed by a ring closure completes the isomerization.

It is difficult to accept formation of intermediate **B**, because the two iron fragments in **B** are connected only by an Fe−Fe bond, which is apparently weaker than Fe−(*μ*-GaMes) and Fe−(*μ*-CO) bonds. This favors path A. Furthermore, it has been proved that [CpFe(CO)]$_2$-(*μ*-CO)(*μ*-$SiMeSiMe_3$), which is closely related to **2b**, undergoes cis−trans isomerization via a mechanism involving formation of a silylene-bridged diiron complex with no Fe−Fe bond as an intermediate.[9b]

Structures of Gallylene-Bridged Diiron Complexes 1a, 2a, and *trans*-2b. To determine the geometric configuration of **2a** and *trans*-**2b**, crystal structure analyses of these complexes were carried out. The X-ray crystal structure of **1a**, which is the starting complex of **2a**, was also determined to clarify the structural difference between complexes **1** and **2**.

Figure 2 shows an ORTEP view of complex **1a**. Selected bond distances and angles are summarized in Table 3. Complex **1a** consists of two well-separated Fp* fragments (Fp* = Cp*Fe(CO)$_2$) with a gallium atom in a trigonal planar configuration. There is a crystal-

Table 3. Selected Bond Lengths [Å] and Angles [deg] for [Cp*Fe(CO)$_2$]$_2$(μ-GaMes) (1a)

Fe−Ga	2.4315(15)	Ga−C13	2.014(10)
Fe−C1	1.736(9)	Fe−C2	1.729(9)
Fe−C3	2.097(8)	Fe−C4	2.088(8)
Fe−C5	2.085(8)	Fe−C6	2.105(7)
Fe−C7	2.137(8)	O1−C1	1.157(8)
O2−C2	1.172(8)		
Fe−Ga−Fe′	124.42(7)	Fe−Ga−C13	117.79(4)
Ga−Fe−C2	78.7(2)	Ga−Fe−C1	85.7(2)
C1−Fe−C2	98.3(4)	Fe−C1−O1	172.9(7)
Fe−C2−O2	175.5(8)		

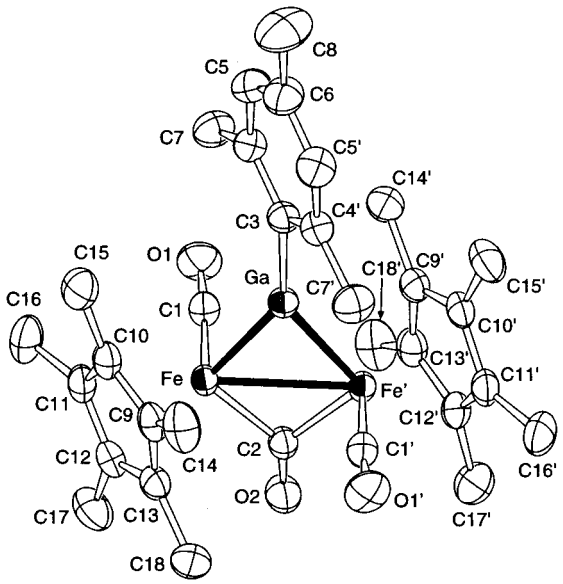

Figure 3. ORTEP drawing (50% probability level) of [Cp*Fe(CO)]$_2$(μ-CO)(μ-GaMes) (**2a**).

lographic 2-fold rotation axis through the Ga, C13, C16, and C18 atoms. The Fe−Ga−Fe′ angle (124.42(7)°) is slightly wider than the Fe−Ga−C13 angle (117.79(4)°). The Fe−Ga distance (2.4315(15) Å) is in the range of usual Fe−Ga single bonds (2.29−2.52 Å)[2,3,13,14] but slightly longer than those in [CpFe(CO)$_2$]$_2$(μ-GaBu^t) (**3**) (2.406(1) and 2.416(1) Å),[2] which is attributable to the steric repulsion between the mesityl group and two bulky Cp* ligands. The interatomic distances between C11 and C17 (3.65(2) Å) and C12 and C17′ (3.51(2) Å) are shorter than the sum of the van der Waals radii of two methyl groups (4.0 Å).

Crystal structure analyses of **2a** (Figure 3, Table 4) and *trans*-**2b** (Figure 4, Table 5) revealed that each complex consists of two Cp′Fe(CO) units bridged by a carbonyl ligand and a mesitylgallylene ligand. As expected from the IR spectroscopic data, **2a** and *trans*-**2b** have trans configuration. In complex **2a**, there is a crystallographic 2-fold rotation axis through the Ga, C3, C6, and C8 atoms; thus, the gallium takes a trigonal

Table 4. Selected Bond Lengths [Å] and Angles [deg] for [Cp*Fe(CO)]$_2$(μ-CO)(μ-GaMes) (2a)

Fe−Fe′	2.7022(11)	Fe−Ga	2.3147(9)
Fe−C1	1.737(2)	Fe−C2	1.932(2)
Fe−C9	2.159(2)	Fe−C10	2.135(2)
Fe−C11	2.093(2)	Fe−C12	2.116(2)
Fe−C13	2.150(2)	Ga−C3	1.976(3)
O1−C1	1.160(3)	O2−C2	1.188(4)
Fe−Ga−Fe′	71.42(4)	Fe−Ga−C3	144.289(19)
Ga−Fe−Fe′	54.289(19)	C2−Fe−Fe′	45.64(7)
C1−Fe−C2	94.78(8)	Ga−Fe−C1	89.92(8)
Ga−Fe−C2	99.93(7)	C1−Fe−Fe′	93.88(8)
Fe−C1−O1	176.0(2)	Fe−C2−O2	135.64(7)
Fe−C2−Fe′	88.72(13)		

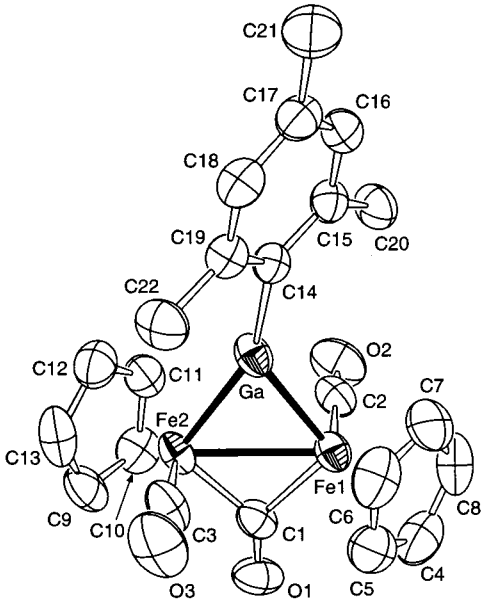

Figure 4. ORTEP drawing (50% probability level) of [CpFe(CO)]$_2$(μ-CO)(μ-GaMes) (*trans*-**2b**).

Table 5. Selected Bond Lengths [Å] and Angles [deg] for [CpFe(CO)]$_2$(μ-CO)(μ-GaMes) (*trans*-2b)

Fe1−Fe2	2.6526(6)	Fe1−Ga	2.3489(6)
Fe2−Ga	2.3438(5)	Fe1−C1	1.900(3)
Fe1−C2	1.749(4)	Fe2−C1	1.935(4)
Fe2−C3	1.740(4)	Ga−C14	1.973(3)
O1−C1	1.195(4)	O2−C2	1.149(5)
O3−C3	1.155(5)		
Fe1−Ga−Fe2	68.840(19)	Fe1−Ga−C14	135.50(9)
Fe2−Ga−C14	153.21(9)	Ga−Fe1−Fe2	55.489(17)
Ga−Fe2−Fe1	55.671(16)	C1−Fe1−Fe2	46.79(11)
C1−Fe2−Fe1	45.69(9)	Ga−Fe1−C1	102.27(11)
Ga−Fe2−C1	101.36(9)	Fe1−C2−O2	178.7(4)
Fe2−C3−O3	177.7(4)	Fe1−C1−O1	136.3(3)
Fe2−C1−O1	136.2(3)	Fe1−C1−Fe2	87.52(14)

planar geometry. The geometry around Ga atom in *trans*-**2b** is, in contrast to **2a**, slightly distorted from the regular trigonal plane (sum of the valence angles around the Ga atom = 357.5(2)°), which is attributable to a weak intermolecular interaction between the gallium atom and an oxygen atom O1 of the bridged carbonyl group in the adjacent molecule. The Ga···O distance (2.956(3) Å) is smaller than the sum of the van der Waals radii of Ga and O (3.39 Å), but significantly longer than that found in CpFe(CO)$_2$GaBu$^t_2$·[CpFe(CO)]$_2$(μ-CO)$_2$ (2.334(9) Å).[2] The latter complex contains a four-coordinate gallium atom; the gallium atom in CpFe(CO)$_2$GaBu$^t_2$ interacts with the oxygen atom of a

(13) Jutzi, P.; Neumann, B.; Reumann, G.; Stammler, H.-G. *Organometallics* **1998**, *17*, 1305.
(14) (a) Vanderhooft, J. C.; Ernst, R. D.; Cagle, F. W., Jr.; Neustadt, R. J.; Cymbaluk, T. H. *Inorg. Chem.* **1982**, *21*, 1876. (b) Green, M. L. H.; Mountford, P.; Smout, G. J.; Speel, S. R. *Polyhedron* **1990**, *9*, 2763. (c) Campbell, R. M.; Clarkson, L. M.; Clegg, W.; Hockless, D. C. R.; Pickett, N. L.; Norman, N. C. *Chem. Ber.* **1992**, *125*, 55. (d) Fischer, R. A.; Priermeier, T.; Scherer, W. *J. Organomet. Chem.* **1993**, *459*, 65. (e) Fischer, R. A.; Miehr, A.; Priermeier, T. *Chem. Ber.* **1995**, *128*, 831. (f) Brothers, P. J.; Power, P. P. *Adv. Organomet. Chem.* **1996**, *39*, 1. (g) Borovik, A. S.; Bott, S. G.; Barron, A. R. *Organometallics* **1999**, *18*, 2668.

bridging CO ligand in $[CpFe(CO)]_2(\mu\text{-}CO)_2$. No interaction of this type was observed in **2a** and **1a**, which is apparently due to the steric crowding around the gallium atom caused by the bulky Cp* and the Mes groups.

The Fe−Ga bond lengths of **2a** (2.3147(9) Å) and *trans*-**2b** (2.3439(6), 2.3438(5) Å) are much shorter than that of **1a** (2.4315(15) Å) and are close to the lower limit of the reported Fe−Ga single bonds (2.29−2.52 Å).[2,3,13,14] These are longer than or comparable to those of the recently reported terminal gallylene−iron complexes $RGaFe(CO)_4$ (2.2248(7) Å for R = 2,6-bis(2,4,6-triisopropylphenyl)phenyl,[15] 2.2731(4) Å for R = Cp*,[13] and 2.315(3) Å for R = tris(3,5-dimethylpyrazolyl)borate[16]). Although Fe−Ga bonds in **2a** and *trans*-**2b** are relatively short compared to the usual Fe−Ga single bonds, π-back-donation from the filled iron d-orbital to the empty gallium p-orbital is insignificant, since the CO stretching frequencies for **2a** (1882 and 1734 cm^{-1}) and *trans*-**2b** (1942, 1905, and 1751 cm^{-1}) are comparable to or even lower than those for the structurally similar silylene- and germylene-bridged diiron complexes, $[Cp'Fe(CO)]_2(\mu\text{-}CO)(\mu\text{-}ERR')$ (Cp′ = Cp, Cp*; E = Si, Ge; R, R′ = Me, Bu^t, *p*-Tol, $SiMe_3$, H) (ν_{CO} 2005−1900 and 1794−1712 cm^{-1}), in which no empty p-orbital is available on the bridging atom to accept electron density from the metal.[9,17] Weakness of the back-donation from the metal to gallium has also been elucidated by the recent MO calculations on the terminal gallylene complexes.[18]

The Fe−Fe bond distances of **2a** (2.7022(11) Å) and *trans*-**2b** (2.6526(6) Å) are much shorter than those of $[Fe(CO)_3]_2\{\mu\text{-}GaSi(SiMe_3)_3\}_3$ (**6**) (2.876(1) Å)[5] and $[Fe(CO)_3]_2\{\mu\text{-}Ga(\eta\text{-}C_5Me_5)\}_2\{\mu\text{-}Ga(\eta^3\text{-}C_5Me_5)\}$ (**10**) (2.908(6) Å),[13] but comparable to those of $[Fe(CO)_3]_2\{\mu\text{-}GaSi(SiMe_3)_3\}_2(\mu\text{-}CO)$ (**7**) (2.6804(8) Å),[5] $[Fe(CO)_3]_3(\mu\text{-}CO)\{\mu\text{-}GaC(SiMe_3)_3\}_2$ (**9**) (2.7785(7), 2.7651(7), 2.6661(8) Å),[6] and a base-coordinated indylene-bridged complex, $[CpFe(CO)]_2(\mu\text{-}CO)(\mu\text{-}In(CH_2)_3NMe_2)$ (2.683(1) Å).[19] The Fe−Ga−Fe′ angles of **2a** (71.42(4)°) and *trans*-**2b** (68.840(19)°) are comparable to those in **6**, **7**, **9**, and **10** (68−74°)[5,6,13] and the Fe−E−Fe (E = Si, Ge) angles of the silylene- and germylene-bridged complexes with a metal−metal bond (65−77°).[1c]

Experimental Section

General Procedures. All manipulations were performed using either standard Schlenk tube techniques under a nitrogen or argon atmosphere, vacuum line techniques, or a drybox under a nitrogen atmosphere. THF, benzene, toluene, and hexane were dried by refluxing over sodium benzophenone ketyl followed by distillation under a nitrogen atmosphere. NaFp[20] and KFp*[21] were prepared by literature procedures. Photolysis was carried out externally with a medium-pressure Hg arc lamp (Ushio UV-450) placed in a water-cooled quartz jacket. The sample tube was immersed in ice−water during the irradiation. The distance from the light source to the sample was ca. 4 cm.

NMR spectra were recorded on a Bruker ARX-300 Fourier transform spectrometer. IR spectra were obtained on a HORIBA FT-200 spectrometer. Mass spectra were recorded on a JEOL HX-110 spectrometer at the Instrumental Analysis Center for Chemistry, Tohoku University, or a Shimadzu GCMS-QP5050A. Elemental analyses were performed at the Instrumental Analysis Center for Chemistry, Tohoku University.

Preparation of $MesGaCl_2$. The title compound was previously prepared by redistribution between Mes_3Ga and $GaCl_3$,[22] but in this study, by the following method. To a stirred solution of $GaCl_3$ (5.1 g, 29 mmol) in hexane (30 mL) was added dropwise a suspension of MesLi (3.7 g, 29 mmol) in hexane (170 mL) at −63 °C. The reaction mixture was stirred for 1 h at −63 °C and for 14 h at room temperature. Volatiles were removed from the reaction mixture under reduced pressure. Molecular distillation of the residue (150 °C/4.0 × 10^{-3} Torr) afforded $MesGaCl_2$ (3.1 g, 12 mmol, 47%).

Synthesis of Fp^*_2GaMes (1a). To $MesGaCl_2$ (1.06 g, 4.09 mmol) was added dropwise a THF solution (60 mL) of KFp* (8.04 mmol) at −48 °C. The reaction mixture was stirred for 1 h at −48 °C and then for 19 h at room temperature. Volatiles were removed from the reaction mixture under reduced pressure. The residue was extracted with 35 mL of toluene, and the extract was filtered through a glass filter. The filtrate was concentrated to ca. 5 mL. Cooling the solution at −30 °C gave yellow crystals of Fp^*_2GaMes (**1a**) (0.979 g, 1.43 mmol, 36%). ^1H NMR (300 MHz, C_6D_6): δ 6.84 (s, 2H, Ar), 2.41 (s, 6H, *o*-CH_3), 2.31 (s, 3H, *p*-CH_3), 1.46 (s, 30H, Cp*). ^{13}C NMR (75.5 MHz, C_6D_6): δ 219.9 (CO), 164.4, 140.1, 136.9, 127.2 ($C_6H_2(CH_3)_3$), 94.0 ($C_5(CH_3)_5$), 23.3 (*o*-CH_3), 21.4 (*p*-CH_3), 9.8 ($C_5(CH_3)_5$). IR (THF): ν_{CO} 1973 (vs), 1942 (w), 1915 (vs), 1900 (w) cm^{-1}. MS (EI, 70 eV): *m*/*z* 682 (M^+, 1), 654 (M^+ − CO, 6), 626 (M^+ − 2CO, 9), 435 (M^+ − Fp*, 100). Anal. Calcd for $C_{33}H_{41}Fe_2GaO_4$: C, 58.02; H, 6.05. Found: C, 58.30; H, 6.20.

Synthesis of Fp_2GaMes (1b). Complex **1b** was synthesized in 82% yield by the reaction of NaFp and $MesGaCl_2$ in a manner similar to that used for **1a**. ^1H NMR (300 MHz, C_6D_6): δ 6.80 (s, 2H, Ar), 4.18 (s, 10H, Cp), 2.31 (s, 6H, *o*-CH_3), 2.23 (s, 3H, *p*-CH_3). ^{13}C NMR (75.5 MHz, C_6D_6): δ 216.3 (CO), 164.4, 137.6, 137.3, 127.4 ($C_6H_2(CH_3)_3$), 82.5 (Cp), 23.0 (*o*-CH_3), 21.3 (*p*-CH_3). IR (THF): ν_{CO} 1996 (s), 1967 (s), 1944 (s, br) cm^{-1}. MS (EI, 70 eV): *m*/*z* 542 (M^+, 1), 514 (M^+ − CO, 1), 486 (M^+ − 2CO, 2), 365 (M^+ − Fp, 78), 309 (M^+ − Fp − 2CO, 60), 121 (CpFe, 100). Anal. Calcd for $C_{23}H_{21}Fe_2GaO_4$: C, 50.89; H, 3.90. Found: C, 51.24; H, 4.08.

Synthesis of $[Cp^*Fe(CO)]_2(\mu\text{-}CO)(\mu\text{-}GaMes)$ (2a). A solution of Fp^*_2GaMes (**1a**) (0.392 g, 0.574 mmol) in toluene (24 mL) was placed into a Pyrex sample tube (o.d. 10 mm) with a Teflon vacuum stopcock and irradiated for 2 h. Progress of the reaction was monitored by ^1H NMR spectroscopy, sampling periodically a small portion of reaction mixture from the reaction vessel. After irradiation, the reaction mixture was concentrated and cooled to −30 °C in a refrigerator to give dark violet crystals of $[Cp^*Fe(CO)]_2(\mu\text{-}CO)(\mu\text{-}GaMes)$ (**2a**) (0.152 g, 0.232 mmol, 40%). ^1H NMR (300 MHz, C_6D_6): δ 6.90 (s, 2H, Ar), 2.79 (s, 6H, *o*-CH_3), 2.23 (s, 3H, *p*-CH_3), 1.71 (s, 30H, Cp*). ^{13}C NMR (75.5 MHz, C_6D_6): δ 288.3 (CO), 215.5 (CO), 155.3, 142.2, 139.7, 128.5 ($C_6H_2(CH_3)_3$), 93.7 ($C_5(CH_3)_5$),

(15) Su, J.; Li, X.-W.; Crittendon, R. C.; Campana, C. F.; Robinson, G. H. *Organometallics* **1997**, *16*, 4511.
(16) Reger, D. L.; Garza, D. G.; Rheingold, A. L.; Yap, G. P. A. *Organometallics* **1998**, *17*, 3624.
(17) (a) Job, R. C.; Curtis, M. D. *Inorg. Chem.* **1973**, *12*, 2514. (b) Tobita, H.; Kawano, Y.; Shimoi, M.; Ogino, H. *Chem. Lett.* **1987**, 2247. (c) Malisch, W.; Ries, W. *Angew. Chem., Int. Ed. Engl.* **1989**, *28*, 5. (d) Tobita, H.; Kawano, Y.; Ogino, H. *Chem. Lett.* **1989**, 2155. (e) Ueno, K.; Hamashima, N.; Shimoi, M.; Ogino, H. *Organometallics* **1991**, *10*, 959. (f) Kawano, Y.; Tobita, H.; Shimoi, M.; Ogino, H. *J. Am. Chem. Soc.* **1994**, *116*, 8575. (g) Kawano, Y.; Sugawara, K.; Tobita, H.; Ogino, H. *Chem. Lett.* **1994**, 293.
(18) (a) Feng, X.; Cotton, F. A. *Organometallics* **1998**, *17*, 128. (b) Boehme, C.; Frenking, G. *Chem. Eur. J.* **1999**, *5*, 2184. (c) Macdonald, C. L. B.; Cowley, A. H. *J. Am. Chem. Soc.* **1999**, *121*, 12213. (d) Uddin, J.; Boehme, C.; Frenking, G. *Organometallics* **2000**, *19*, 571.
(19) Fischer, R. A.; Herdtweck, E.; Priermeier, T. *Inorg. Chem.* **1994**, *33*, 934.
(20) King, R. B.; Pannell, K. H.; Bannett, C. R.; Ishaq, M. *J. Organomet. Chem.* **1969**, *19*, 327.
(21) Cathelin, D.; Astruc, D. *Organometallics* **1984**, *3*, 1094.
(22) Beachley, O. T., Jr.; Churchill, M. R.; Pazik, J. C.; Ziller, J. W. *Organometallics* **1987**, *6*, 2088.

Table 6. Crystal Data and Structure Refinement for [Cp*Fe(CO)$_2$]$_2$(μ-GaMes) (1a), [Cp*Fe(CO)]$_2$(μ-CO)(μ-GaMes) (2a), and [CpFe(CO)]$_2$(μ-CO)(μ-GaMes) (*trans*-2b)

	1a	2a	*trans*-2b
empirical formula	$C_{33}H_{41}Fe_2GaO_4$	$C_{32}H_{41}Fe_2GaO_3$	$C_{22}H_{21}Fe_2GaO_3$
fw	683.08	655.07	514.81
cryst syst	tetragonal	monoclinic	monoclinic
space group	$I4_1/a$ (variant of No. 88)	$C2/c$ (No. 15)	$P2_1/c$ (No. 14)
unit cell dimens	a = 14.484(8) Å c = 31.703(15) Å	a = 14.090(6) Å b = 17.178(9) Å c = 12.532(4) Å β = 99.59(3)°	a = 8.5605(3) Å b = 19.6762(8) Å c = 12.8157(5) Å β = 106.460(3)°
volume	6651(6) Å^3	2991(2) Å^3	2070.19(14) Å^3
Z	8	4	4
density (calcd)	1.364 g/cm^3	1.455 g/cm^3	1.652 g/cm^3
abs coeff	1.698 mm^{-1}	1.882 mm^{-1}	2.694 mm^{-1}
F(000)	2832	1360	1040
cryst size	0.30 × 0.30 × 0.30 mm	0.30 × 0.30 × 0.30 mm	0.4 × 0.3 × 0.2 mm
θ range for data collection	1.55−27.50°	1.89−27.51°	1.95−27.48°
index ranges	$0 \le h \le 18$, $0 \le k \le 18$, $-41 \le l \le 0$	$-18 \le h \le 18$, $0 \le k \le 22$, $-16 \le l \le 0$	$-11 \le h \le 11$, $-25 \le k \le 25$, $-16 \le l \le 16$
no. of reflns collected	4130	3615	18 789
no. of ind reflns	3832 [R(int) = 0.0626]	3456 [R(int) = 0.0183]	4701 [R(int) = 0.0497]
no. of reflns with $I > 2\sigma(I)$	1367	2746	3920
abs corr	ψ-scan	ψ-scan	integration
max. and min. transmn	1.0000 and 0.8797	0.9998 and 0.9718	0.6418 and 0.5293
refinement method	full-matrix least-squares on F^2	full-matrix least-squares on F^2	full-matrix least-squares on F^2
no. of data/restraints/params	3832/0/190	3456/0/252	4701/0/253
goodness-of-fit on F^2	0.933	1.021	1.142
final R indices [$I > 2\sigma(I)$][a]	R1 = 0.0629, wR2 = 0.1087	R1 = 0.0276, wR2 = 0.0674	R1 = 0.0382, wR2 = 0.1093
R indices (all data)[a]	R1 = 0.2371, wR2 = 0.1543	R1 = 0.0451, wR2 = 0.0737	R1 = 0.0508, wR2 = 0.1220
largest diff peak and hole	0.335 and −0.327 e Å^{-3}	0.276 and −0.294 e Å^{-3}	0.573 and −0.639 e Å^{-3}

[a] $R1 = \sum||F_o| - |F_c||/\sum|F_o|$ and $wR2 = [\sum[w(F_o^2 - F_c^2)^2]/\sum[w(F_o^2)^2]]^{1/2}$.

23.9 (*o*-CH_3), 21.5 (*p*-CH_3), 9.8 ($C_5(CH_3)_5$). IR (C_6D_6): ν_{CO} 1882 (vs), 1734 (vs) cm^{-1}. MS (EI, 70 eV): *m*/*z* 654 (M^+, 25), 626 (M^+ − CO, 18), 598 (M^+ − 2CO, 8), 435 (M^+ − 3CO, 5), 435 (M^+ − Cp*FeCO, 32), 379 (Cp*FeGaMes, 100). Anal. Calcd for $C_{32}H_{41}Fe_2GaO_3$: C, 58.67; H, 6.31. Found: C, 58.94; H, 6.09.

Synthesis of [CpFe(CO)]$_2$(μ-CO)(μ-GaMes) (2b). Complex **2b**, which is a mixture of *cis*-**2b** and *trans*-**2b**, was obtained in 66% yield by photolysis of Fp_2GaMes (**1b**) in a manner similar to that used for **2a**. ^{1}H NMR (300 MHz, C_6D_6): δ 6.84 (s, 2H, Ar, *trans*-**2b**), 6.81 (s, 2H, Ar, *cis*-**2b**), 4.29 (s, 10H, Cp, *trans*-**2b**), 4.14 (s, 10H, Cp, *cis*-**2b**), 2.58 (s, 6H, *o*-CH_3, *trans*-**2b**), 2.47 (s, 6H, *o*-CH_3, *cis*-**2b**), 2.21 (s, 3H, *p*-CH_3, *trans*-**2b**), 2.20 (s, 3H, *p*-CH_3, *cis*-**2b**). ^{13}C NMR (75.5 MHz, C_6D_6): δ 279.2, 278.0 (CO), 212.7, 212.4 (CO), 156.6, 154.5, 141.7, 140.9, 140.4, 140.0, 128.1, 127.8 ($C_6H_2(CH_3)_3$), 82.3, 81.7 (Cp), 24.0, 23.9 (*o*-CH_3), 21.39, 21.36 (*p*-CH_3). IR (THF): ν_{CO} 1942 (vs), 1905 (vs), 1751 (vs) cm^{-1}. MS (EI, 70 eV): *m*/*z* 514 (M^+, 30), 486 (M^+ − CO, 35), 458 (M^+ − 2CO, 10), 430 (M^+ − 3CO, 30), 361 (Cp_2Fe_2Mes, 35), 309 (CpFeGaMes, 100), 296 ($CpFe_2Mes$, 20). Anal. Calcd for $C_{22}H_{21}Fe_2GaO_3$: C, 51.33; H, 4.11. Found: C, 51.06; H, 4.24.

Isolation of *trans*-[CpFe(CO)]$_2$(μ-CO)(μ-GaMes) (*trans*-2b). The isomer mixture of **2b** (0.030 g, 0.058 mmol) was dissolved into a mixed solvent of toluene (1 mL) and hexane (1 mL) at room temperature. The solution was kept at −30 °C for 1 week. Dark violet crystals of pure *trans*-**2b** were obtained in 43% yield (0.013 g, 0.025 mmol).

Kinetic Study of the Cis−Trans Isomerization of [CpFe(CO)]$_2$(μ-CO)(μ-GaMes) (2b). Crystals of *trans*-**2b** (ca. 10 mg) were placed in an NMR sample tube connected to a vacuum line via a ground glass joint. Toluene-d_8 (0.4 mL) was transferred into the sample tube by a conventional trap-to-trap method. The sample tube was then flame sealed. The isomerization reaction was monitored periodically by ^{1}H NMR spectroscopy at 273, 278, 283, 288, and 293 K. The molar ratio of each isomer was determined from the intensities of ^{1}H NMR signals of *o*-Me groups. A linear correlation was found between $\ln(A_t - A_\infty/A_0 - A_\infty)$ and time, where A_0, A_t, and A_∞ are molar fractions of *trans*-**2b** at time 0, *t*, and infinite, respectively. The rate constants, k_1 and k_{-1}, were calculated from the slope of the plot, which corresponds to $-(k_1 + k_{-1})$, and equilibrium constant K = [cis]/[trans] = k_1/k_{-1} at the observed temperature (Table 1). Activation parameters, $\Delta H^\ddagger$ and $\Delta S^\ddagger$, were obtained from the Eyring plot and are summarized in Table 2.

X-ray Crystal Structure Determination of 1a, 2a, and *trans*-2b. A single crystal of **1a**, **2a**, or *trans*-**2b** was sealed into a glass capillary under an atmosphere of dry nitrogen. The intensity data for X-ray crystal structure analyses were collected on a RIGAKU AFC-6A four-circle diffractometer for **1a** and **2a** and a RIGAKU RAXIS-RAPID imaging plate diffractometer for *trans*-**2b** with graphite-monochromated Mo Kα radiation at 293 K. The observed data were corrected for Lorentz and polarization effects. Semiempirical absorption corrections based on the ψ scans were applied for the data of **1a** and **2a**, whereas numerical absorption corrections for *trans*-**2b**. The space groups, $I4_1/a$ for **1a**, $C2/c$ for **2a**, and $P2_1/c$ for *trans*-**2b**, were determined on the basis of the systematic absence and the subsequent least-squares refinement. Crystallographic data for **1a**, **2a**, and *trans*-**2b** are listed in Table 6. The structures were solved by Patterson and Fourier transform methods (SHELXS-97).[23] All non-hydrogen atoms were refined by full-matrix least-squares techniques with anisotropic displacement parameters based on F^2 with all reflections (SHELXL-97).[24] All hydrogen atoms were placed at their geometrically calculated positions and refined riding on the corresponding carbon atoms with isotropic thermal parameters ($U = 1.5U(C_{methyl})$ and $1.2U(C_{methyne})$). Calculations for **1a** and **2a** and that of *trans*-**2b** were performed on an Apple Macintosh computer and a Silicon Graphics O_2 computer, respectively.

Acknowledgment. The authors thank Dowa Mining Co., Ltd. for a gift of $GaCl_3$. This work was supported

(23) Sheldrick, G. M. *SHELXS-97, Program for Crystal Structure Determination*; University of Göttingen: Göttingen, Germany, 1997.
(24) Sheldrick, G. M. *SHELXL-97, Program for Crystal Structure Determination*; University of Göttingen: Göttingen, Germany, 1997.

by a Grant-in-Aid for Scientific Research (No. 11640554) from the Ministry of Education, Science, Sports and Culture of Japan.

Supporting Information Available: Tables giving crystal data, atomic coordinates and equivalent isotropic displacement parameters of non-hydrogen atoms, bond lengths and angles, anisotropic displacement parameters, and hydrogen coordinates and isotropic displacement parameters for **1a**, **2a**, and *trans*-**2b**. This material is available free of charge via the Internet at http://pubs.acs.org.

OM000675A